

# 73 GHz Millimeter Wave Propagation Measurements for Outdoor Urban Mobile and Backhaul Communications in New York City

George R. MacCartney Jr.  
NYU WIRELESS

NYU Polytechnic School of Engineering  
Brooklyn, NY 11201  
gmac@nyu.edu

Theodore S. Rappaport  
NYU WIRELESS

NYU Polytechnic School of Engineering  
Brooklyn, NY 11201  
tsr@nyu.edu

**Abstract**—The spectrum congestion experienced in today's common cellular bands has led to research and measurements to explore the vast bandwidths available at millimeter waves (mmWaves). NYU WIRELESS conducted E-band propagation measurements for both mobile and backhaul scenarios in 2013 in the dense urban environment of New York City using a sliding correlator channel sounder, by transmitting a 400 Mega chip per second (Mcps) PN sequence with a power delay profile (PDP) multipath time resolution of 2.5 ns. Measurements were made for more than 30 transmitter-to-receiver location combinations for both mobile and backhaul scenarios with separation distances up to 200 m. This paper presents results that support the use of directional steerable antennas at mmWave bands in order to achieve comparable path loss models and channel statistics to today's current cellular systems and at 28 GHz. These early results reveal that the mmWave spectrum, specifically the E-band, could be used for future cellular communications by exploiting multipath in urban environments with the help of beam-steering and beam combining.

**Index Terms**—mmWave; 5G; E-band; sliding correlator; channel sounder; path loss; 73 GHz; propagation; directional steerable antennas;

## I. INTRODUCTION

The technological advancements of smartphones, tablets, and other devices have created an increase in the demand of data and mobile network access. This demand has put a burden on cellular service providers and network engineers to meet the growing needs of customers, with a minimal amount of bandwidth available [1]. Presently, many service providers use piecemeal techniques and complex coding schemes to afford enough bandwidth to barely meet the current data demands. This technique involves using fragmented parts of the spectrum, as it is rare for carriers to operate over large contiguous bandwidths due to licensing and ownership. The re-farming of older 2G and GSM bands has opened up some spectrum space for LTE and 4G, but this makes piecemeal spectrum allocation techniques more complex for cellular operators [2]. As the density of devices in urban cells continues to grow, channel capacities are reaching their limits; therefore, researchers are currently exploring solutions to this spectrum

shortfall. Because most of the spectrum is currently licensed or allocated for specific uses, unused bands and frequencies with large bandwidths are a promising solution. Specifically, the mmWave bands are looked to as a potential solution for future mobile and backhaul wireless communications due to the large contiguous bandwidths available, the development of cheap CMOS integrated circuits, and on-chip antennas [3]–[10].

The mmWave bands were once an afterthought for cellular because of the perceived increase in oxygen absorption and rain attenuation compared with today's cellular bands. However, researchers have shown that at the mmWave bands of 28 GHz, 38 GHz, and the 73 GHz E-band, there will be a negligible degree of atmospheric attenuation for inter-site distances up to 200 m [3], [5], [10], [11]. In addition, researchers have shown for heavy rainfall of 25 mm/hr, that attenuation is only 1.4 dB for 28 GHz, 1.6 dB for 38 GHz, and 2 dB for 73 GHz at distances of 200 m [3], [5], [10], [11]. Inter-site distances of 200 m will be common for future systems, as many of today's femto and picocells have maximum inter-site distances of 100 to 150 m [12]. In addition to negligible atmospheric attenuation comparable to today's current cellular bands for small inter-site distances, mmWave frequencies offer an enormous amount of unused, and in some cases, unlicensed spectrum. The E-band alone has two contiguous bandwidths of 5 GHz available between 71-76 GHz and 81-86 GHz that could be used for future 5G cellular and backhaul [5], [13]. Nokia Solutions and Networks is predicting a 10,000 fold increase in network capacity by 2025 that must be met with solutions outside of the current cellular bands, and the bandwidths available at E-band frequencies are a worthwhile avenue to explore in order to meet this increase [6].

Academic researchers have recently conducted extensive measurement campaigns in the mmWave spectrum to gain a better understanding of propagation characteristics and its viability for the future of 5G communications systems [3], [4], [10], [11]. The goal of the measurements is to use reliable data to accurately model the statistics of the mmWave bands for key parameters including path loss, delay spread, number of mul-

tipath components, and angles of arrival (AoA) and departure (AoD) to develop temporal and spatial channel models that are fundamental in helping engineers with designing future generations of wireless systems. [3], [4], [10], [11], [14], [15]. Researchers at NYU WIRELESS conducted a measurement campaign in the Summer of 2013 in New York City at 73 GHz, very similar to the campaign conducted in 2012 at 28 GHz [3], [10], [14]. Measurements were conducted for both line of sight (LOS) and non-line-of-sight (NLOS) conditions for transmitter (TX) and receiver (RX) separation distances up to 200 m. There were a total of 9 LOS and 74 NLOS TX-RX combinations tested. For these scenarios, LOS measurements refer to the TX and RX antennas perfectly aligned boresight-to-boresight, with no obstructions between them. The NLOS conditions include obstructions by large city buildings that do not allow for a point-to-point link between the TX and RX as well as measurements with no obstructions but where the TX and RX antennas are not perfectly boresight-to-boresight.

## II. 73 GHz E-BAND CHANNEL SOUNDER HARDWARE

Similar to the channel sounder used for measurements in [3], [5], [10], [14], a 400 Mega chip per second (Mcps) spread spectrum sliding correlator channel sounder is used to test and measure the 73 GHz outdoor radio mobile and backhaul channel. The channel was measured by transmitting and receiving an 11th order pseudorandom m-sequence centered at 73.5 GHz with a broadband 800 MHz first null-to-null RF bandwidth. The baseband 400 MHz clocked signal is first mixed with an intermediate frequency (IF) of 5.625 GHz,

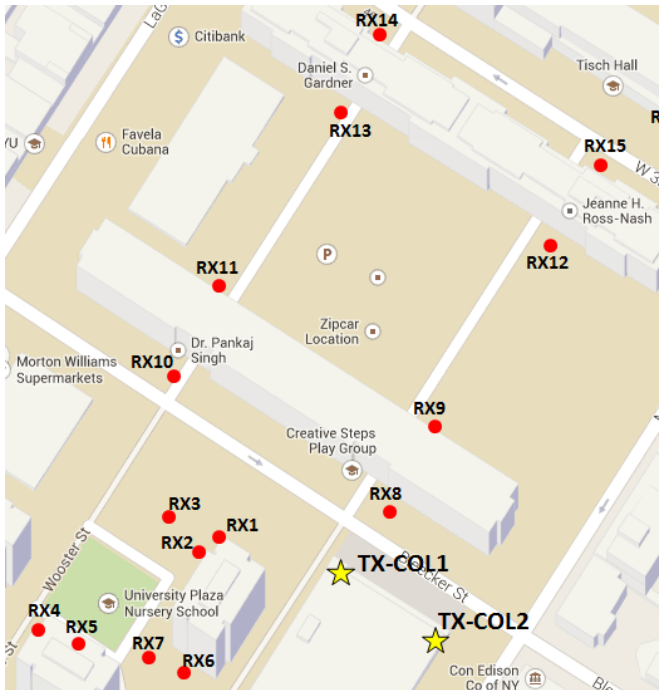


Fig. 1: Map showing backhaul and mobile RX locations around NYU’s campus for the 2 TX locations used on top of the Coles Sports Center. The TX locations are identified as stars, and the RX locations are identified as circles.

TABLE I: 73 GHz Outdoors Sliding Correlator Channel Sounder Specifications

<b>Carrier Frequency</b>	73.5 GHz
<b>TX PN Code Chip Rate</b>	400 Mcps
<b>RX PN Code Chip Rate</b>	399.95 Mcps
<b>Slide Factor <math>k</math></b>	8000
<b>TX Power</b>	14.6 dBm
<b>EIRP</b>	41.6 dBm
<b>RX Antenna</b>	27 dBi 7° half-power beamwidth Vertically Polarized
<b>TX Antenna</b>	27 dBi 7° half-power beamwidth Vertically Polarized
<b>Maximum Measurable Path Loss (5 dB SNR)</b>	181 dB
<b>Multipath Time Resolution</b>	2.5 ns
<b>Maximum Measurable Excess Delay</b>	1800 ns

and is then upconverted with a driving local oscillator (LO) frequency of 67.875 GHz (via a frequency-tripled 22.625 GHz signal) to transmit the ultra wide spread spectrum sequence at an RF center frequency of 73.5 GHz. Both the TX and RX systems of the channel sounder used compact National Instruments QuickSyn digitally tuned frequency oscillators rather than large signal generators for ease of transportation. At the receiver, PDPs are recorded at incremental steps in the azimuth plane as explained further in Section III. Both the TX and RX used rotatable 27 dBi horn antennas with 7° half-power beamwidths in the azimuth and elevation planes, with vertical polarization. The TX transmitted the PN sequence at a power of 14.6 dBm for a total EIRP of 41.6 dBm when considering the TX antenna gain. The channel sounder at the RX produced the same 11th order PN sequence as the TX, but clocked at a slightly slower rate of 399.95 MHz to create a slide factor of 8000 [16]–[18]. Using 27 dBi antennas at the TX and RX, and post-processing, our system provides a total measurable path loss of 181 dB, operating at a 5 dB SNR threshold.

## III. 73 GHz E-BAND CHANNEL SOUNDER MEASUREMENT PROCEDURE

Outdoor ultra wideband measurements at 73 GHz were conducted around New York University’s (NYU) downtown Manhattan campus. Measurements in downtown Manhattan provide a multipath rich urban environment. Both backhaul-to-backhaul and base-station-to-mobile measurements were conducted for TX and RX inter-site distance combinations between 30 and 200 meters. 200 meters was chosen as the maximum distance because of limited TX power, and based on prior measurement results at 28 GHz. In addition, to support user demand and to achieve greater channel capacity, it is predicted that future mmWave wireless systems in a dense urban environment will provide access points on every street

73 GHz Path Loss Vs. Distance with RX Height: 2 m  
Using 27 dBi, 7° 3dB BW TX and RX Antennas in Manhattan

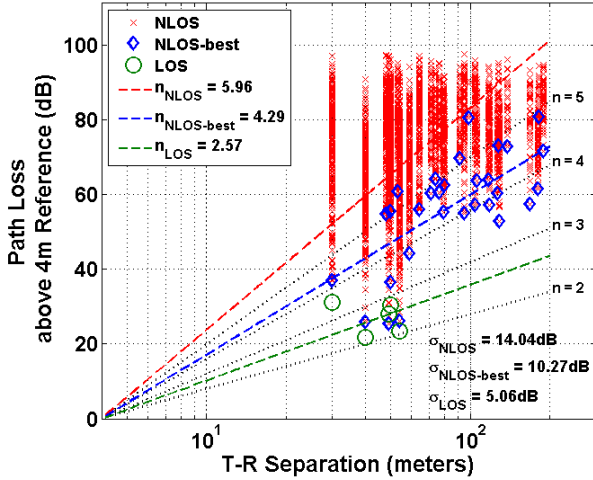


Fig. 2: New York City mobile height (2m) path losses at 73 GHz as a function of T-R separation distance using vertically polarized 27 dBi, 7° half-power beamwidth TX & RX antennas. All data points represent path loss values calculated from recorded PDP measurements. Red crosses indicate all NLOS pointing angle data points, blue diamonds indicate best NLOS pointing angle data points for each T-R combination, and green circles indicate LOS data points. The measured path loss values are relative to a 4 m free space close-in reference distance. NLOS PLEs are calculated for the entire data set and also for the best recorded link. LOS PLEs are calculated for strictly boresight-to-boresight scenarios.  $n$  values are PLEs and  $\sigma$  values are shadow factors.

73 GHz Path Loss Vs. Distance with RX Height: 4.06 m  
Using 27 dBi, 7° 3dB BW TX and RX Antennas in Manhattan

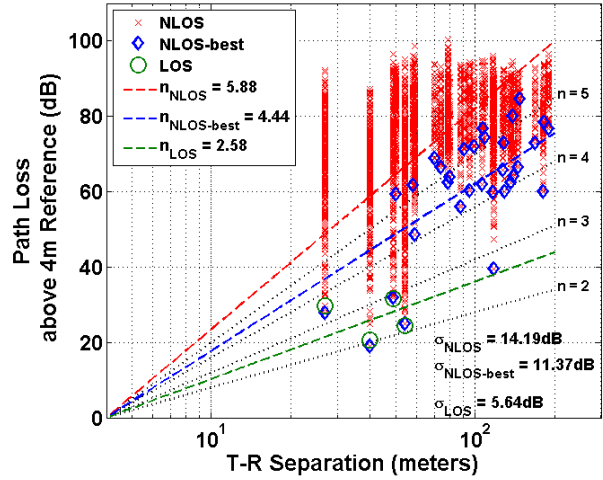


Fig. 3: New York City backhaul height (4m) path losses at 73 GHz as a function of T-R separation distance using vertically polarized 27 dBi, 7° half-power beamwidth TX & RX antennas. All data points represent path loss values calculated from recorded PDP measurements. Red crosses indicate all NLOS pointing angle data points, blue diamonds indicate best NLOS pointing angle data points for each T-R combination, and green circles indicate LOS data points. The measured path loss values are relative to a 4 m free space close-in reference distance. NLOS PLEs are calculated for the entire data set and also for the best recorded link. LOS PLEs are calculated for strictly boresight-to-boresight scenarios.  $n$  values are PLEs and  $\sigma$  values are shadow factors.

corner or lamppost [3], [6], [11], [15]. Two TX locations were chosen on the rooftop of NYU’s Coles Sports Center at heights of 7 meters above ground, two TX locations were on the 2nd floor balcony of the Kimmel Center at heights of 7 meters above ground, and one TX location was chosen on the 5th floor balcony of the Kaufman building at a height of 17 meters above ground level. For the Coles Sports Center transmitters, 15 RX locations were selected in the surrounding campus and city blocks at heights of 2 meters (mobile) and 4.06 meters (backhaul) relative to the ground. For the Kaufman building TX, 11 RX locations were chosen for both mobile and backhaul scenarios. Based on access approved by NYU and NYPD officials, a total of 36 TX-RX combinations were measured for mobile scenarios and 38 TX-RX combinations were measured for backhaul scenarios, for a total of 74 TX-RX combination scenarios, but some of these combinations resulted in outages. Because LOS conditions are less common and less available in dense-urban scenarios, a majority of TX-RX links were in NLOS conditions. The RX locations were pseudorandomly selected based on approval and AC outlet accessibility. Fig. 1 shows a map of RX measurement locations for both the COL1 and COL2 TX locations on top of the Coles Sports Center.

For each TX-RX scenario combination, many different pointing angle combinations were measured. In LOS scenarios, the boresight-to-boresight pointing direction between the TX and RX antennas was always the strongest link. However,

this is not the case for NLOS environments. At the beginning of each measurement day for each location, both the TX and RX antennas were exhaustively rotated in both the azimuth and elevation planes to find the strongest received signal power at the RX. Once this angle combination was determined, the TX antenna remained fixed and the RX antenna was mechanically rotated in the 360° azimuth plane using FLIR gimbals that offered 1/3 of a degree pointing accuracy with repeatability. In LOS scenarios, the RX antenna was stepped in 10° increments, and in NLOS scenarios, the RX antenna was stepped in 8° increments. At each step increment where the received power was noticeable above the noise floor of the RX system, a power delay profile was recorded. A full azimuth sweep is counted as one measurement configuration.

Measurement configurations were then conducted for variations in the elevation plane for both the TX and RX antennas, such that the RX elevation was fixed to +/- one beamwidth in the elevation plane for two azimuth plane sweeps and then the TX antenna elevation was fixed to +/- one beamwidth in the elevation plane for two RX antenna azimuth sweeps. This resulted in five initial measurement configurations. Next, two TX azimuth sweeps were conducted with the RX antenna fixed in the two strongest azimuth and elevation pointing angles respectively found during the initial five RX azimuth sweeps. After the completion of two TX antenna sweeps, up to five more RX antenna sweeps were performed in the same manner as the first five, however a new main angle of departure at the

TX antenna was selected based on information obtained from the two TX antenna sweeps. This resulted in up to 12 overall measurement configurations per TX-RX combination, both for mobile and backhaul scenarios. Thus, for one mobile or backhaul NLOS TX-RX location combination, up to 450 PDPs were recorded over the period of a half a day to a full day. Each measured PDP consisted of an average of 20 consecutive instantaneous PDPs which took approximately 0.8 seconds to record. The RX antenna sweeps are important for AoA statistics, and the TX antenna sweeps are important for AoD statistics that provide insight for a statistical spatial channel model using lobe theory [14], [15]. Table I lists the settings and configurations of the channel sounder system. Small-scale measurements were not taken, as small-scale fading appears to be negligible at mmWaves [3], [10].

#### IV. 73 GHZ E-BAND URBAN MICROCELLULAR PROPAGATION RESULTS AND ANALYSIS

In order to understand and model the 73 GHz E-Band channel, initial calculations were done to quantify the path loss of the transmitted signal as a function of distance with the commonly used close-in reference distance model represented in Eq. 1:

$$\overline{PL}(d)[dB] = PL_{fs}(d_0)[dB] + 10\bar{n} \log_{10} \left( \frac{d}{d_0} \right) + X_{\sigma} \quad (1)$$

where  $\overline{PL}(d)$  is the average path loss in dB for a specific T-R separation distance of  $d$  in meters,  $d_0$  is the close-in free space reference distance,  $\bar{n}$  is the average path loss exponent for the entire data set of measurement configurations, and  $X_{\sigma}$  is a Gaussian random variable with 0 dB mean and standard deviation  $\sigma$  in dB [16]. The close-in reference free space path loss is defined by Eq. 2:

$$PL_{fs}(d_0)[dB] = 20 \log_{10} \left( \frac{4\pi d_0}{\lambda} \right) \quad (2)$$

This free space leverage point model offers slightly higher (less than 0.5 dB) standard deviation than an arbitrary curve fit, but offers important physical meaning [11], [15]. For all of the measurements in this paper, a 4 m close-in reference distance is used, as this is in the far-field region of both horn antennas. Of the 74 TX-RX location combinations, 12 resulted in an outage (no received signal). LOS and NLOS data are calculated separately, considering TX antenna heights were lumped together to find the initial PLEs (path loss exponents). Figs. 2 and 3 show the computed path losses for all combined PDP measurements recorded for the mobile and backhaul scenarios, respectively. LOS measurements include the environment where the transmitter and receiver antennas are perfectly boresight-to-boresight with no obstructions between the link. The LOS links for the mobile scenario resulted in a PLE with  $\bar{n} = 2.57$  and a shadow factor of 5.06 dB. This PLE is greater than  $n = 2$  for theoretical free space, likely due to the fact that achieving perfect boresight-to-boresight alignment at large distances with tight beamwidth antennas is extremely difficult. Improvements have been made to the measurement

TABLE II: 73 GHz PLE and SF For Backhaul and Mobile where ‘best’ refers to the best TX-RX pointing angle,  $d_0 = 4m$

	Transmitter height of 7 meters					
	73 GHz Backhaul-to-Backhaul			73 GHz Base Station-to-Mobile		
	# of RXs	PLE	SF (dB)	# of RXs	PLE	SF (dB)
LOS	2	2.68	6.79	3	2.77	5.33
NLOS	21	6.06	14.44	18	6.33	13.29
NLOS Best	21	4.72	9.52	18	4.64	8.32
	Transmitter height of 17 meters					
	73 GHz Backhaul-to-Backhaul			73 GHz Base Station-to-Mobile		
	# of RXs	PLE	SF (dB)	# of RXs	PLE	SF (dB)
LOS	2	2.52	4.00	2	2.32	2.71
NLOS	11	5.70	13.51	11	5.52	12.86
NLOS Best	11	3.90	10.81	11	3.76	8.81

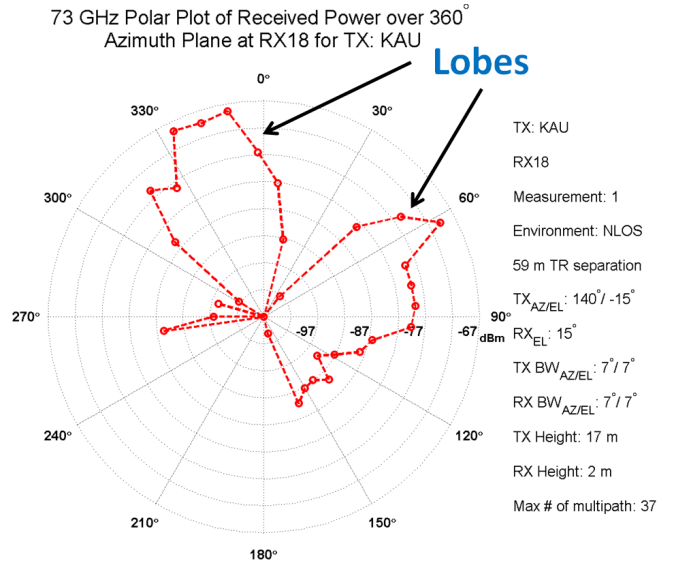


Fig. 4: Polar plot displaying the received power in a NLOS environment for the TX at a height of 17 meters and the RX at a mobile height of 2 meters for a T-R separation distance of 59 meters in New York City. Each dot corresponds to the total received power over an 8° angular resolution. This polar plot shows the diverse amount of AoAs that can be used for beam combining and beamforming in NLOS environments for the future of mmWave 5G wireless communications. Two lobes are observed, corresponding to main incoming directions of arrival where received energy is contiguous in both time and space. The 0° orientation refers to the receiver facing true North.

system to include laser pointers for better boresight accuracy in the future. The NLOS data included radio paths with building obstructions and scenarios where there was light foliage between the TX and RX antennas, that can result in an additional loss of approximately 20 dB at mmWaves [19]. For mobile NLOS scenarios without considering specific TX

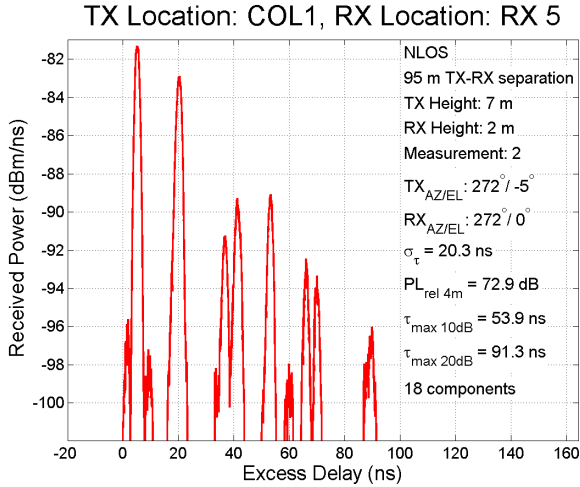


Fig. 5: PDP recorded at a NLOS mobile RX location for a TX at 7 meters above ground on top of Coles Sports Center in New York City. The separation distance between the TX and RX is 95 meters. This PDP has 18 detectable multipath components with maximum excess delay spread of 91.3 ns for the component 20 dB down from the first arriving multipath component.  $\sigma_\tau$  is the RMS delay spread of the PDP.

antenna heights, and averaged over all pointing angles when some energy could be detected, the overall PLE was 5.96 with a shadow factor of 14.04 dB. This result is slightly worse than values determined at 28 GHz in New York City [10] as well as PLEs determined in the semi-urban environment of Austin, Texas for rooftop-to-ground and peer-to-peer measurements [3], [10], [11], [20], [21] in the 38 GHz and 60 GHz mmWave bands. Fig. 3 shows the path losses calculated for each measurement with the RX antenna at a height of 4.06 meters in order to simulate a backhaul-to-backhaul urban microcellular environment. The overall NLOS PLE for the backhaul scenario for all pointing angles that yielded received energy is 5.88 with a shadow factor of 14.19 dB. The large NLOS PLE and standard deviation about the mean path loss value is a result of many different paths of great dynamic range supported over a wide range of angles in the dense urban environment of New York City. The large buildings on every city block and crowded streets create numerous blockages, reflections, and scatterers between the transmitter and receiver. These values are surprisingly comparable to those found by NYU WIRELESS in New York City at 28 GHz [10], but with slightly more path loss and slightly fewer multipath components [15].

While overall PLEs are important for understanding propagation, more valuable PLEs can be generated when considering different TX-RX antenna heights, as the shadow factor or standard deviation of path loss values about the mean path loss has been shown to vary based on elevation and antenna tilt [14], [22]. For the measurements conducted in New York City at 73 GHz, two different TX antenna heights were used for mobile and backhaul measurements. Table II shows the LOS and NLOS PLEs calculated for both mobile and backhaul scenarios with TX-RX antenna height diversity. It is apparent

from Table II that backhaul and mobile RX antenna heights for the higher TX antenna height of 17 m have comparable PLE results.

Millimeter wave wireless will rely on multipath rich environments and directional antennas to overcome additional propagation losses at mmWave frequencies. An azimuthal 360° polar plot in a typical NLOS environment from the measurement campaign is displayed in Fig. 4. Each dot in Fig. 4 represents the total integrated received power at the corresponding azimuth angle. This plot illustrates a reflective and multipath-rich environment in which directions of arrival may be found at many possible azimuth angles at the RX for a fixed TX azimuth angle. This information can be used to combine multipath components from different AoAs in order to improve the PLEs through both beam combining or beamforming. Work in [23], [24] has shown the improvement in PLEs for beam combining both coherently and non-coherently at 28 GHz in New York City, and this method may also be applied to 73 GHz. Fig. 5 shows a typical PDP and observed multipath delay spread for a NLOS environment during the 73 GHz measurement campaign. This PDP and Fig. 4 reveal that multipath signals can be combined through beamforming and beam combining for significant improvements in link margin. The plot shows that the maximum excess delay spread 20 dB down from the first arriving multipath component is 91.3 ns while the RMS delay spread is 20.3 ns, indicating the need for channel equalization in conjunction with beam combining. This PDP shows that even for tight 7° beamwidth antennas at the TX and RX, the environment is rich in multipath components that can be combined to increase the received power of the signal.

## V. CONCLUSION

This paper presents what we believe to be the world's first E-band wideband propagation measurements at 73 GHz in New York City for backhaul and mobile wireless communication channels using steerable, 27 dBi 7° half-power beamwidth antennas. Overall, 74 TX-RX link combinations were measured in both elevation and azimuth planes for backhaul and mobile scenarios, although 12 combinations resulted in outage. Without TX antenna height diversity, the LOS PLE  $\bar{n}$  was found to be 2.57 for the mobile scenario and 2.58 for the backhaul scenario. In addition, the NLOS PLE  $\bar{n}$  was reduced from 5.96 to 4.29 when considering the best link (e.g. best pointing direction for TX and RX antennas) for the mobile scenario, and was reduced from 5.88 to 4.44 for the backhaul scenario, respectively. These results show directional antennas make mmWave wireless viable, and further work is developing omnidirectional models with measured data at 28 and 73 GHz [15]. The omnidirectional model presented in [15] shows that path losses at these mmWave bands are much higher than today's UHF and microwave bands. However, beamforming can lower these path losses with directional antennas. Combining the best directional links can further reduce the PLE as shown in [23], [24]. It is also apparent that without TX antenna height diversity, the PLE is more favorable for the backhaul scenario.

This is most likely due to the elevated RX antenna height that allows for more unobstructed and reflected paths between the TX and RX antennas. When considering the best received links using directional antennas, the PLEs are comparable to today's current UHF and microwave cellular PLEs in the dense urban environment.

For inter-site distances within 200 meters, mmWaves are a potential solution for the growing need for bandwidth. This measurement campaign reveals that, by taking advantage of the rich multipath environment with beam combining and beamforming, steerable antennas and chip antenna arrays can be developed in order to achieve more than reasonable radio links [4], [7], [8]. The 5-10 GHz of available bandwidth in the E-band spectrum should be considered as a solution to meet the increasing demand of bandwidth and higher data rates by mobile users as current capacity becomes limited. With the small wavelengths at mmWaves, smaller base-station units may be deployed to offer end-user and backhaul connectivity on every street corner or lamppost in urban city environments.

## VI. ACKNOWLEDGEMENT

This project was sponsored by Nokia Solutions and Networks and the GAANN Fellowship program. The authors wish to thank Rimma Mayzus, Hannar J. Lee, Abhi Shah, Shu Sun, Mathew K. Samimi, and Shuai Nie of NYU WIRELESS for their contributions to the measurements, and the NYU Administration, NYU Public Safety, and the NYPD for their support of this measurement campaign. This project was also supported by the following NYU WIRELESS Industrial Affiliates: Samsung, National Instruments, Qualcomm, L-3 Communications, Huawei, NSN, Intel, and AT&T.

## REFERENCES

- [1] Z. Pi and F. Khan, "An introduction to millimeter-wave mobile broadband systems," *Communications Magazine, IEEE*, vol. 49, no. 6, pp. 101–107, June 2011.
- [2] R. D. Vieira, R. C. D. Paiva, J. Hultkonen, R. Jarvela, R. F. Iida, M. Saily, F. Tavares, and K. Niemela, "GSM evolution importance in re-farming 900 MHz band," in *Vehicular Technology Conference Fall (VTC 2010-Fall)*, 2010 IEEE 72nd, Sept 2010, pp. 1–5.
- [3] T. S. Rappaport, S. Sun, R. Mayzus, H. Zhao, Y. Azar, K. Wang, G. N. Wong, J. Schulz, M. Samimi, and F. Gutierrez, "Millimeter wave mobile communications for 5G cellular: It will work!" in *Access, IEEE*, vol. 1, 2013, pp. 335–349.
- [4] T. S. Rappaport, F. Gutierrez, E. Ben-Dor, J. N. Murdock, Y. Qiao, and J. I. Tamir, "Broadband millimeter-wave propagation measurements and models using adaptive-beam antennas for outdoor urban cellular communications," in *Antennas and Propagation, IEEE Transactions on*, vol. 61, no. 4, April 2013, pp. 1850–1859.
- [5] S. Nie, G. R. MacCartney, S. Sun, and T. S. Rappaport, "72 GHz millimeter wave indoor measurements for wireless and backhaul communications," in *Personal Indoor and Mobile Radio Communications (PIMRC)*, 2013 IEEE 24th International Symposium on, Sept 2013, pp. 2429–2433.
- [6] Nokia Solutions and Networks, "2020: Beyond 4G radio evolution for the gigabit experience," 2011.
- [7] L. Ragan, A. Hassibi, T. S. Rappaport, and C. L. Christianson, "Novel on-chip antenna structures and frequency selective surface (FSS) approaches for millimeter wave devices," in *Vehicular Technology Conference, 2007. VTC-2007 Fall. 2007 IEEE 66th*, Sept 2007, pp. 2051–2055.
- [8] F. Gutierrez, S. Agarwal, K. Parrish, and T. S. Rappaport, "On-chip integrated antenna structures in CMOS for 60 GHz WPAN systems," *Selected Areas in Communications, IEEE Journal on*, vol. 27, no. 8, pp. 1367–1378, October 2009.
- [9] T. S. Rappaport, R. W. Heath Jr., R. Daniels, and J. N. Murdock, *Millimeter Wave Wireless Communications*. Pearson Prentice Hall, 2014.
- [10] Y. Azar, G. N. Wong, K. Wang, R. Mayzus, J. K. Schulz, H. Zhao, F. Gutierrez, D. Hwang, and T. S. Rappaport, "28 GHz propagation measurements for outdoor cellular communications using steerable beam antennas in new york city," in *International Conference on Communications (ICC)*, 2013 IEEE, June 2013, pp. 5143–5147.
- [11] G. R. MacCartney, J. Zhang, S. Nie, and T. S. Rappaport, "Path loss models for 5G millimeter wave propagation channels in urban microcells," in *Global Communications Conference (GLOBECOM)*, 2013 IEEE, Dec 2013.
- [12] D. Lopez-Perez and X. Chu, "Inter-cell interference coordination for expanded region picocells in heterogeneous networks," in *Computer Communications and Networks (ICCCN)*, 2011 Proceedings of 20th International Conference on, July 2011, pp. 1–6.
- [13] FCC 03-248, "Allocation and services for the 71-76 GHz, 81-86 GHz and 92-95 GHz bands," Nov 2003.
- [14] M. Samimi, K. Wang, Y. Azar, G. N. Wong, R. Mayzus, H. Zhao, J. K. Schulz, S. Sun, F. Gutierrez, and T. S. Rappaport, "28 GHz angle of arrival and angle of departure analysis for outdoor cellular communications using steerable beam antennas in new york city," in *Vehicular Technology Conference (VTC Spring)*, 2013 IEEE 77th, June 2013, pp. 1–6.
- [15] S. Rangan, T. S. Rappaport, and E. Erkip, "Millimeter wave cellular wireless networks: potentials and challenges," *Proceedings of the IEEE*, (to appear) 2014.
- [16] T. S. Rappaport, *Wireless Communications: Principles and Practice*, 2nd ed. Upper Saddle River, NJ: Prentice Hall, 2002.
- [17] D. Cox, "Delay doppler characteristics of multipath propagation at 910 MHz in a suburban mobile radio environment," *Antennas and Propagation, IEEE Transactions on*, vol. 20, no. 5, pp. 625–635, Sep 1972.
- [18] G. Martin, "Wideband channel sounding dynamic range using a sliding correlator," in *Vehicular Technology Conference Proceedings, 2000. VTC 2000-Spring Tokyo. 2000 IEEE 51st*, vol. 3, 2000, pp. 2517–2521 vol.3.
- [19] S. Joshi and S. Sancheti, "Foliage loss measurements of tropical trees at 35 ghz," in *Recent Advances in Microwave Theory and Applications, 2008. MICROWAVE 2008. International Conference on*, Nov 2008, pp. 531–532.
- [20] E. Ben-Dor, T. S. Rappaport, Y. Qiao, and S. J. Lauffenburger, "Millimeter-wave 60 GHz outdoor and vehicle AOA propagation measurements using a broadband channel sounder," in *Global Telecommunications Conference (GLOBECOM 2011)*, 2011 IEEE, Dec 2011, pp. 1–6.
- [21] T. S. Rappaport, E. Ben-Dor, J. N. Murdock, and Y. Qiao, "38 GHz and 60 GHz angle-dependent propagation for cellular and peer-to-peer wireless communications," in *International Conference on Communications (ICC)*, 2012 IEEE, June 2012, pp. 4568–4573.
- [22] D. Kifle, B. Wegmann, I. Viering, and A. Klein, "Impact of antenna tilting on propagation shadowing model," in *Vehicular Technology Conference (VTC Spring)*, 2013 IEEE 77th, June 2013, pp. 1–5.
- [23] S. Sun, G. R. MacCartney, M. Samimi, S. Nie, and T. S. Rappaport, "Millimeter wave multi-beam antenna combining for 5G cellular link improvement," in *International Conference on Communications (ICC)*, 2014 IEEE, June 2014.
- [24] S. Sun and T. S. Rappaport, "Multi-beam antenna combining for 28 GHz cellular link improvement in urban environments," in *Global Communications Conference (GLOBECOM)*, 2013 IEEE, Dec 2013.